The nature of the X-ray transient MAXI J0556−332

R. Cornelisse[1,2]⋆, P. D'Avanzo[3], S. Campana[3], J. Casares[1,2], P.A. Charles[4,5],
G. Israel[6], T. Muñoz-Darias[3], K. O'Brien[7], D. Steeghs[8], L. Stella[6], M.A.P. Torres[9]

[1] *Instituto de Astrofisica de Canarias, Via Lactea, La Laguna E-38200, Santa Cruz de Tenerife, Spain*
[2] *Departamento de Astrofisica, Universidad de La Laguna, E-38205 La Laguna, Tenerife, Spain*
[3] *INAF- Osservatorio Astronomico di Brera, via E. Bianchi 46, 23807 Merate, Italy*
[4] *South Africa Astronomical Observatory, P.O. Box 9, Observatory 7935, South Africa*
[5] *School of Physics and Astronomy, University of Southampton, Highfield, Southampton SO17 1BJ, UK*
[6] *INAF-Osservatorio Astronomico di Roma, Via Frascati 33, I-00040 Monteporzio Catone (Rome), Italy*
[7] *Department of Physics, University of California, Santa Barbara, CA, USA*
[8] *Department of Physics, University of Warwick, Coventry, CV4 7AL, UK*
[9] *SRON, Netherlands Institute for Space Research, Sorbonnelaan 2, 3584 CA, Utrecht, The Netherlands*

ABSTRACT
Phase-resolved spectroscopy of the newly discovered X-ray transient MAXI J0556−332 has revealed the presence of narrow emission lines in the Bowen region that most likely arise on the surface of the mass donor star in this low mass X-ray binary. A period search of the radial velocities of these lines provides two candidate orbital periods (16.43±0.12 and 9.754±0.048 hrs), which differ from any potential X-ray periods reported. Assuming that MAXI J0556−332 is a relatively high inclination system that harbors a precessing accretion disk in order to explain its X-ray properties, it is only possible to obtain a consistent set of system parameters for the longer period. These assumptions imply a mass ratio of $q \simeq 0.45$, a radial velocity semi-amplitude of the secondary of $K_2 \simeq 190$ km s^{-1} and a compact object mass of the order of the canonical neutron star mass, making a black hole nature for MAXI J0556−332 unlikely. We also report the presence of strong N III emission lines in the spectrum, thereby inferring a high N/O abundance. Finally we note that the strength of all emission lines shows a continuing decay over the $\simeq 1$ month of our observations.

Key words: accretion, accretion disks – stars:individual (MAXI J0556−332) – X-rays:binaries.

1 INTRODUCTION

Amongst the brightest objects in the X-ray sky are the low mass X-ray binaries (LMXBs), exotic systems where the primary is a compact object (either a neutron star or black hole) and the secondary a low-mass ($<1M_\odot$) star. Since the secondary is overflowing its Roche-Lobe, matter is accreted via an accretion disk onto the compact object, giving rise to the observed X-rays. The majority of these LMXBs, the so-called X-ray transients, only show sporadic X-ray activity, but most of the time remain in a state of low-level activity, referred to as quiescence (see e.g. Psaltis 2006 for an overview and more detailed references).

Due to reprocessing of the X-rays, mainly in the outer accretion disk, a LMXB also becomes much brighter in the optical during a transient outburst (e.g. Charles & Coe

2006). Unfortunately, this reprocessed emission completely dominates the optical light, making radial velocity studies using spectral features from the donor star impossible in most cases, while during their quiescent state most transients become too faint for such studies. A powerful alternative method of investigation was opened when Steeghs & Casares (2002) detected narrow emission line components that originated from the irradiated face of the donor star in Sco X-1. These narrow features were most obvious in the Bowen blend (NIII λ4634/4640 and CIII λ4647/4650), which is the result of UV fluorescence from the hot inner disk, and gave rise to the first radial velocity curve of the mass donor in Sco X-1. Thus far, high resolution phase-resolved spectroscopic studies have revealed these narrow lines in more than a dozen optically bright LMXBs, including several transients during their outburst, leading (for most of them) to the first constraint on the mass of the compact object (see Cornelisse et al. 2008 for an overview).
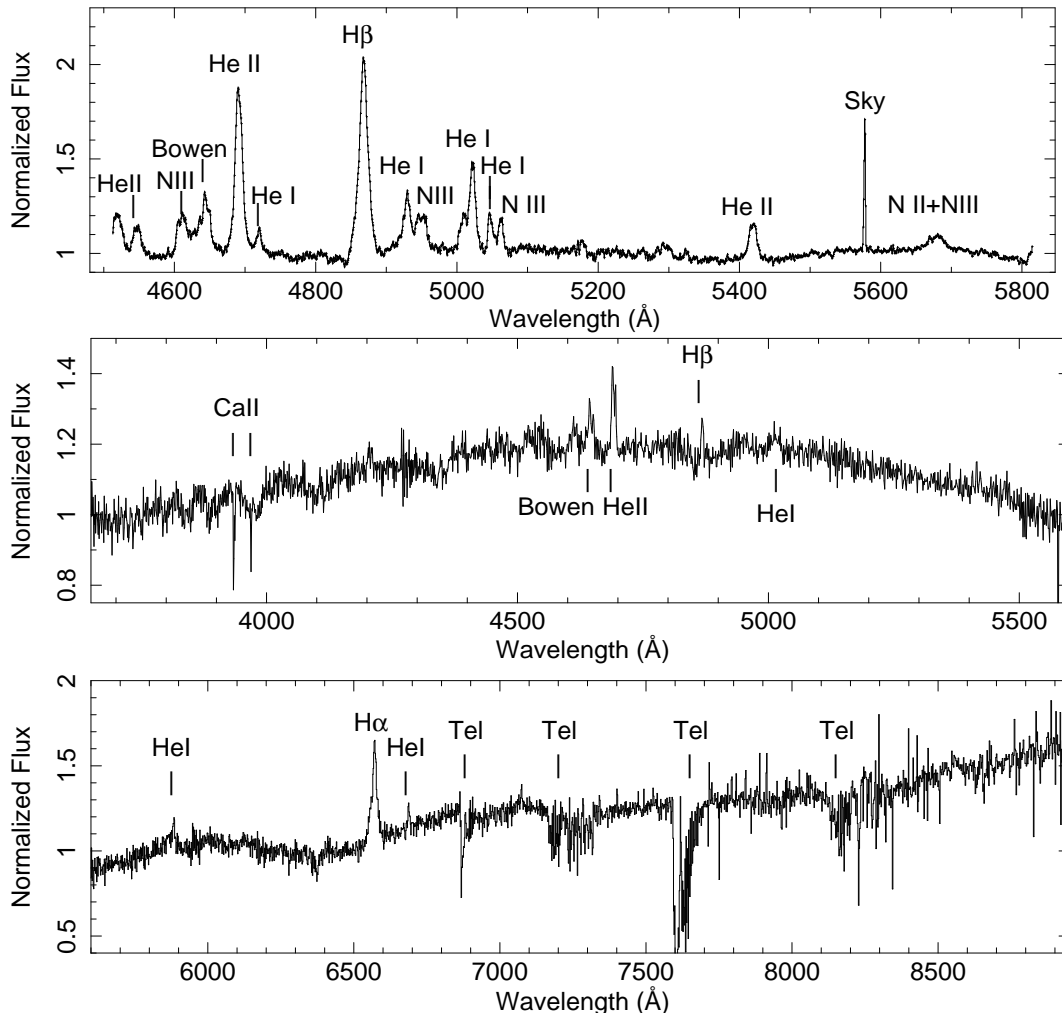
⋆ E-mail: corneli@iac.es

Figure 1. Average flux normalized spectrum of MAXI J0556 obtained with FORS (top) and X-Shooter (middle and bottom). The X-Shooter spectrum is split into two panels, with the top showing the spectrum obtained with the "UBV" arm the middle panel the "VIS" arm. Indicated in both spectra are the most prominent emission lines detected, and we have also indicated the most prominent Telluric absorption features with "Tel".

On January 11 2011 the X-ray transient MAXI J0556−332 (hereafter MAXI J0556) was newly discovered by MAXI/GSC (Matsumura et al. 2011), and quickly thereafter localized by the Swift X-ray telescope (Kennea et al. 2011). Eclipse-like features in the X-ray light-curves led to several possible orbital periods (Strohmayer 2011, Maitra et al. 2011a). Although follow-up X-ray observations excluded all except one (9.33 hr) of these periods (Belloni et al. 2011), further observations were also able to discard this period (Belloni private communication). The optical counterpart was quickly confirmed by Halpern (2011) as an $R \simeq 17.8$ object, making it an excellent target for high resolution spectroscopy. Initial studies of the X-ray spectral and timing variations were unable to indicate the nature of the compact object in MAXI J0556 (Belloni et al. 2011), but more detailed studies by Homan et al. (2011) suggest that its behavior is similar to some of the neutron stars at high accretion rates (the so-called Z-sources). Together with its optical and radio properties this strongly

suggests that MAXI J0556 harbors a neutron star (Russell et al. 2011; Coriat et al. 2011).

In order to identify the nature of MAXI J0556 using the narrow components in the Bowen region we triggered our Target of Opportunity (ToO) observations using FORS 2 on the Very Large Telescope (VLT) and complemented it with Directors Discretionary Time (DDT) using X-Shooter, which is also on the VLT. In this paper we present the results of these observations. In Sect. 2 we discuss the observations in detail, and in Sect. 3 we show the results. We finish with a discussion in Sect. 4 and present further evidence that MAXI J0556 is most likely a neutron star LMXB.

2   OBSERVATIONS AND DATA REDUCTION

On 20 January 2011 we triggered our ToO to observe MAXI J0556 over a period of ≃3 weeks using the FORS 2 instrument on the ESO/VLT. For each exposure we used the 1400V volume-phased holographic grism with a slit width

Table 1. Observation log of MAXI J0556. Indicated are the observing dates and times, instrument used (Setting), integration time for each spectrum (Int.), number of spectra obtained during each night (No,) and the variation of the seeing during these observations (as measured by the DIMM on Paranal).

Date (yy-mm-dd)	Time (UT)	Setting	Int. (s)	No.	Seeing (arcsec)
2011-01-19	00:44-04:50	FORS	671	20	0.45-0.97
2011-01-21	00:54-01:51	FORS	671	4	0.95-1.14
2011-01-22	00:57-01:52	FORS	671	4	0.39-0.45
2011-01-23	00:41-01:37	FORS	671	4	0.74-0-98
2011-01-24	00:50-01:45	FORS	671	4	0.46-0.62
2011-01-25	02:38-03:32	FORS	671	4	0.39-0.77
2011-02-07	00:48-02:19	FORS	671	7	0.47-0.62
2011-02-14	00:28-01:22	X-Shooter	595	4	1.34-1.69
2011-02-14	03:45-04:39	X-Shooter	595	4	0.79-1.02

Table 2. Overview of the average Equivalent Width (EW) of He IIλ4686 and Hβ, the two most prominent emission lines in the FORS spectra, during each observing night. Also listed is the corresponding B magnitude from the acquisition images obtained at the beginning of each block of FORS observations. Also included, as the final entry, are the EW measurements from the average X-Shooter spectrum.

Date (yy-mm-dd)	EW He II (Å)	EW Hβ (Å)	Magnitude B
2011-01-19	4.32±0.02	6.15±0.02	17.1±0.1
2011-01-21	3.42±0.03	5.61±0.03	17.0±0.1
2011-01-22	2.82±0.02	3.19±0.02	17.1±0.1
2011-01-23	2.00±0.03	2.81±0.03	16.9±0.1
2011-01-24	1.86±0.03	2.64±0.03	17.0±0.1
2011-01-25	1.83±0.02	3.31±0.03	17.0±0.1
2011-02-07	1.19±0.02	0.79±0.02	16.4±0.1
2011-02-14	1.04±0.06	0.25±0.06	–

of 0.7″, leading to a wavelength coverage of $\lambda\lambda$4512-5815 with a resolution of 87 km s^{-1} (FWHM). Furthermore, these observations were complemented with 2×1 hr of X-Shooter DDT observations (also located on the VLT). Although both blocks were observed on the same night (14 February 2011), they were separated by several hours. For the X-Shooter observations, which cover the full UV-optical-IR wavelength band, we used a 1.0" slit for the UBV arm (and 0.9" for the other two arms), resulting in a resolution of 66 km s^{-1} (FWHM) around the Bowen region. In Table 1 we give an overview of the observations.

For the FORS observations we de-biased and flat-fielded all the images and used optimal extraction techniques (from the PAMELA software package) to maximize the signal-to-noise ratio of the extracted spectra (Horne 1986). Wavelength calibration was performed using the daytime He, Ne, Hg and Cd arc lamp exposures. We determined the pixel-to-wavelength scale using a 4th order polynomial fit to 10 reference lines giving a dispersion of 0.64 Å pixel^{-1} and rms scatter <0.01 Å. The X-Shooter observations were reduced using the pipeline v.1.2.2 provided by ESO (see Goldoni et al. 2006 for more information), resulting in three 1-dimensional spectra (for each arm of the instrument) per exposure that were flux calibrated using a flux standard obtained during the same night. For the corresponding analysis of the full dataset we used the MOLLY package.

Finally, we reduced our B-band acquisition images from the FORS observations using standard reduction techniques (i.e. performed bias subtraction and flat-fielding). For each image the exposure time was 5 seconds. We only had one image at the start of each observing block, resulting in a total of 7 images. From the reduced images we performed a photometric calibration against the USNO B-band measurements from nearby stars, and list the results in Table 2. We note that for our X-Shooter observations we only have a g' broad band image, and have not included its magnitude in the Table.

3 DATA ANALYSIS

3.1 Spectrum

First we present the average normalized UV-optical spectrum of MAXI J0556 obtained by X-Shooter (top and middle panels) and FORS 2 (bottom) in Fig. 1, and have indicated the most prominent lines. The IR arm of X-Shooter was completely dominated by noise, and we therefore did not include this part of the spectrum in Fig. 1. This figure emphasizes the remarkable contrast in emission line strength between the FORS and X-Shooter observations. In the latter only the most prominent emission lines that are typically observed in LMXBs (i.e the Balmer and He lines and also the Bowen blend) are present, but they are much weaker than during the FORS observations.

For our first observation, the wealth of emission lines in the average FORS spectrum shown in Fig. 1, we start by noting that the typical emission lines for LMXBs (i.e. Hβ, He II λ4686, Bowen and all He I lines) are all present. Furthermore, there are several other emission lines which are not commonly observed in LMXBs. Although these uncommon lines become fainter as a function of time in a similar way to Hβ and He II λ4686 (see above), they appear to be present in all spectra. We therefore conclude that they are real and not an artifact of our reduction. In order to identify these lines, we first moved the average spectrum in such a way that the central wavelength of several He I lines corresponded to their rest-wavelength. Using an atomic line list by van Hoof & Verner (1997) we then noted that most of the uncommon emission lines correspond to the strongest N III or N II transitions or their multiplets. We therefore tentatively conclude that all these lines are due to N III or N II and have indicated them as such in Fig. 1.

Also, given the suggestion by Maitra et al. (2011b) that MAXI J0556 could have an extremely high N/O abundance, we also checked for the presence of strong O and C lines by cross-correlating the line list obtained from ultra-compact C/O binaries by Nelemans et al. (2004). This shows that only C IIIλ4652, which is typically the strongest C or O line in most X-ray binaries (see e.g. Steeghs & Casares 2002),
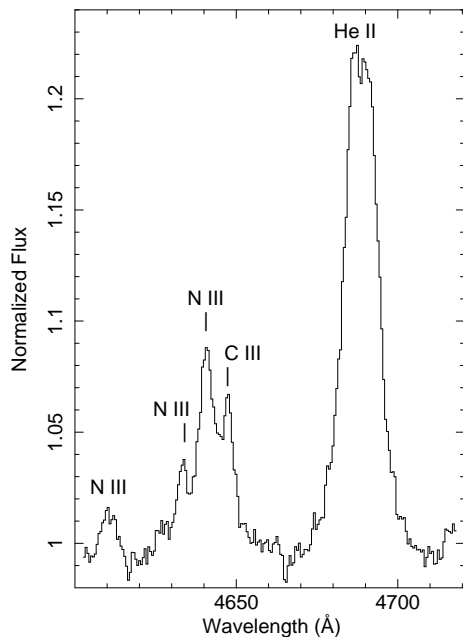
Figure 2. Average spectrum of MAXI J0556 around the He II $\lambda4685.75$ and Bowen region, in the rest frame of the donor star. The indicated narrow components detected in the Bowen region are N III $\lambda4610.55/4610.75$ (not visible in the individual spectra), N III $\lambda4634.12$, N III $\lambda4640.64$ and C III $\lambda4647.42$.

Figure 3. Lomb-Scargle periodogram of all our observations of MAXI J0556. We have indicated the 3σ and 5σ significance levels. Indicated with an X are the proposed X-ray periods by Strohmayer (2011) and the corresponding periods (in days) of the 4 highest peaks. Note that from our first block of FORS observations we can rule out any frequency $\geqslant 5$ cycles per day (see Sect. 3.2).

is clearly present and its relative strength is comparable to that of other X-ray binaries.

In order to understand our second observation, the much weaker emission lines in the X-Shooter, we examined the average FORS spectra for each individual night in more detail. We note that there is a large variability in the emission lines from night to night. In order to quantify this variability we averaged all our spectra during an observing night together and measured the Equivalent Width (EW) of the two strongest emission lines (i.e. He II$\lambda4686$ and Hβ) and list the result in Table 2. Interestingly, the EW for both lines shows a decreasing trend as a function of time (with the exception of Hβ during January 25), while the B-band magnitude stays more or less constant (except during the last FORS observation). Although this decrease in EW resembles a power-law decay, almost all individual points strongly deviate from their best power-law fit, and we decided against providing any fit results. We conclude that the strength of the emission lines in MAXI J0556 is independent of the continuum flux, and show a continuing decay over the $\simeq 1$ month of our observations.

3.2 Radial Velocities

A close inspection of the Bowen region shows that it consists of several narrow components, and in Fig. 2 we show a close-up of this region. In most individual spectra we could identify two (sometimes three) individual components. Following previous observations of the Bowen region (see e.g. Cornelisse et al. 2008 for an overview) we identified the strongest component with N III $\lambda4640.64$ and the second strongest as C III $\lambda4647.42$. In the cases that a third component was present this was identified as N III $\lambda4634.12$, but
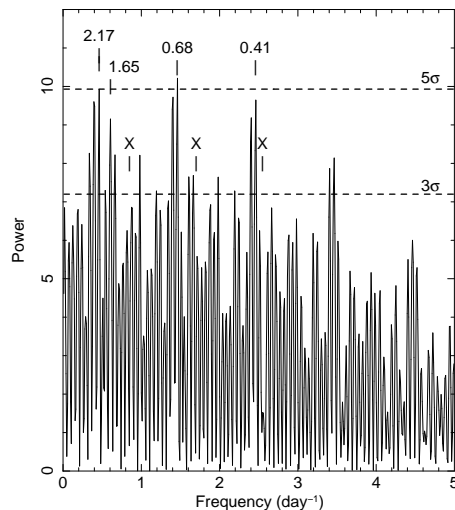
we could not find evidence for C III $\lambda4650.2$, a line that was clearly detected in e.g. Sco X-1 (Steeghs & Casares 2002).

The narrow components in the Bowen region showed clear velocity shifts from night to night. In order to obtain radial velocities from them we averaged two consecutive FORS spectra together to increase the signal-to-noise, while for the X-Shooter spectra we averaged all spectra from the same observing block. This provided a total of 26 spectra from which radial velocities could be measured (note that only the very last spectrum of FORS was not grouped with any other spectrum). Following Steeghs & Casares (2002) we fitted the narrow components with 3 Gaussians (N III$\lambda4634.12/4640.64$ and C III$\lambda4647.42$) under the assumption that they all have a common radial velocity but an independent strength. Using a least squares technique we determined the best common radial velocity and corresponding error.

In order to constrain the orbital period we performed a period analysis on the derived radial velocities using the Lomb-Scargle method (Scargle 1982), which is best suited for unevenly sampled time-series. In Fig. 3 we show the resulting periodogram where we have indicated the 4 strongest peaks that represent good candidates for the orbital period (note that most are related to each other due to the daily alias).

To estimate the significance of the peaks in the periodogram we performed a Monte-Carlo simulation, using identical temporal sampling as for the original radial velocity measurements. Furthermore, our simulations used a distribution and mean of radial velocities that was similar to the original dataset. We produced 500,000 random radial velocity datasets and measured the peak power from the corresponding periodograms. From the distribution of the peak powers we estimated both the 3σ and 5σ confidence levels and have indicated these in Fig. 3. The only periods that have a significance $\geqslant 5\sigma$ are 2.17 and 0.68 days, and we
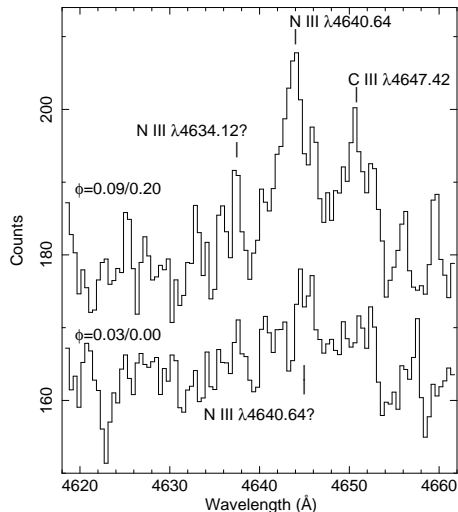
Figure 4. Average spectrum of the first (bottom) and second (top) X-Shooter observations showing a close-up of the Bowen region. We list the corresponding orbital phases for a 1.65 day (first) and 0.68 day (second) orbital period for each block, and have indicated the most prominent narrow components. Note that the narrow components are shifted from their rest-wavelength due to radial velocity motion, and the lines indicated with a question mark are too noisy for unambiguous identification as a true narrow component.

Figure 5. Phase-folded radial velocity curve of MAXI J0556 obtained from the narrow Bowen components for an orbital period of 0.68d (top) and 0.41d (bottom). For clarity, each curve is shown twice.

note that the (almost significant) 0.41 day period is related via the daily alias to the other two significant periods.

First of all we note that none of the suggested X-ray periods by Strohmayer (2011) fit our data. Furthermore, our first block of 20 FORS spectra consisted of 3.7 hrs of continuous observations, with radial velocity measurements that only show an increasing trend and a total amplitude of $\simeq$60 km s^{-1}. Since this amplitude is much smaller than what is observed from night to night ($\simeq$200 km s^{-1}) we conclude that the orbital period must be longer than 0.2 days. Also, the spectra in Fig. 1 show strong Hydrogen lines, thereby excluding an ultra-compact nature of MAXI J0556 and hence any period $\leqslant$1 hr (i.e. close to the integration time of our spectra) as was suggested by Maitra et al. (2011b). We therefore conclude that one of the periods indicated in Fig. 3 is likely to be the true orbital period.

We also looked in more detail at the two blocks of X-Shooter observations, and Fig. 4 shows the average spectrum around the Bowen region of both blocks. We note that the narrow lines, in particular N III λ4640, are almost absent during the first block but have become stronger during the second (while the strength of emission lines such as Hβ and He II λ4686 have not changed significantly). In order to explain this change in the narrow components in only a few hours, we estimated (for the 4 potential orbital periods listed in Fig. 3) the orbital phases for both blocks of X-Shooter observations. First of all we note that that for all orbital periods the first block was obtained around orbital phase 0 (i.e. when the donor star is closest to us). However, the second block was taken around orbital phase 0.25-0.35 for the shorter periods (0.68 and 0.41 days), but is still around phase 0 for the longer periods (2.17 and 1.65 days).
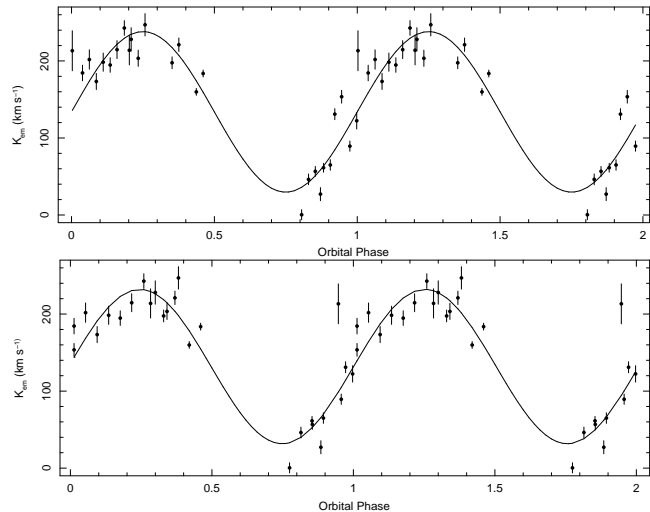
Under the assumption that the narrow components in the Bowen region arise on the irradiated surface of the donor star and the inclination is relatively high (see Sect. 4), the simplest way to explain the change in line strength between the two blocks of X-Shooter observations is that our view of the irradiated surface has changed. Since the first block was obtained around orbital phase 0, the irradiated side should be least visible, and this could explain the weakness of the narrow lines. To explain the increase in line strength, the second block must then have been observed at a significantly different orbital phase where our view of the irradiated surface must have improved. Since the orbital phase only changes significantly between the X-Shooter blocks for the shorter orbital periods (0.68 and 0.41 days), we conclude that the orbital period must be one of these two. Combined with the fact that the timing of the eclipse-like features (see Sect. 4 for a discussion on their nature) also suggests a period $\leqslant$1.2 days, we propose that the true orbital period is either 0.684$\pm$0.005 or 0.406$\pm$0.002 days.

Unfortunately it is not possible to distinguish between these two final candidate periods and we assume that both are equally likely. In Fig. 5 we show the phase-folded radial velocity curve for both candidate periods, and in Table 3 we list the best fitting parameters of their radial velocity curves.

Finally, due to the highly variable nature of the line profiles and strengths of He II λ4686 and Hβ (see Table 2 and also illustrated in Fig. 6) we did not attempt to obtain an estimate of the radial velocity semi-amplitude of the compact object. However, we do point out that both lines appear to be red-shifted compared to the narrow lines in the Bowen region. Whereas N III λ4641 shows a systemic velocity of 130 km s^{-1} (slightly dependent on the assumed period, see Table 3), He II shows a mean velocity of 340 km s^{-1} and for Hβ it is already 400 km s^{-1}. Whereas for Hβ such behavior has been observed before (see e.g. Cornelisse et al. 2007), and could be due to the presence of other non-resolved emission lines, it is uncommon for He II. Since the lines do not appear to be asymmetric and there is also no indication for
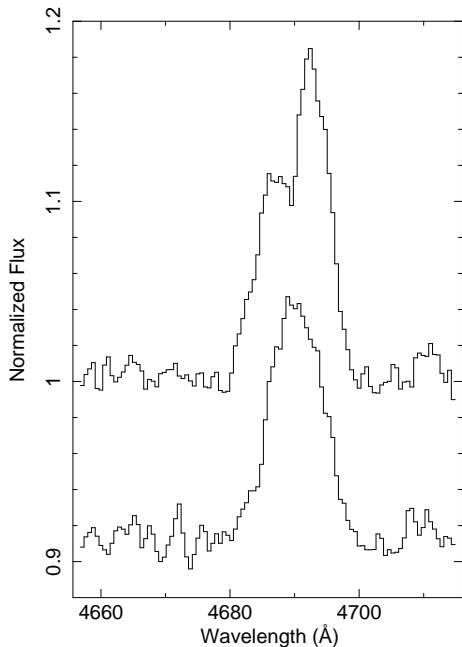
Figure 6. Close-up of the average He II $\lambda 4686$ emission line for two different observing nights. Both observations were obtained at similar orbital phases (for a 0.68d and 0.41d period), but show different line profiles and strengths, Note that for illustration purposes we have off-set the spectra from each other.

the presence of a P Cygni-like profile, we currently do not have a good explanation for this shift.

4   DISCUSSION

We obtained optical spectroscopic observations of MAXI J0556 during its outburst in 2011 and have shown that the average spectrum is not only dominated by strong H, He emission lines but also N. Although the presence of Hydrogen does rule out an ultra-compact nature as was suggested by Maitra et al. (2011b), it does support their suggestion that MAXI J0556 has an unusually high N/O abundance.

Another interesting result is the power-law decay of all the emission lines over the time-span of our observations. This decay appears to be in contradiction with the results by Fender et al. (2009), which showed an anti-correlation between the EW of Hα and the continuum emission. However, they were concerned with the fading phase of the transient outburst, while our observations are mainly during the peak of the outburst. It is interesting to note that in Fig. 2 of Fender et al. (2009) the Hα EW during the peak of the outburst also appears to be dropping for most transients. Fender et al. (2009) provide several explanations, and most of them can also be adopted here. For example, it could be possible that the outer accretion disk becomes hotter over time, thereby changing the optical depth of the emission lines, although saturation effects that hamper the production of the emission lines or even spectral and geometrical changes cannot be ruled out.

Furthermore we have detected narrow Bowen lines in the optical spectrum that moved from night to night. Fol-

Table 3. Overview of the system parameters of MAXI J0556 for both candidate orbital periods. T_0 indicates the time of inferior conjunction of the donor star.

	16 hrs	9.75 hrs
$P_{\rm orb}$ (day)	0.684(5)	0.406(2)
T_0 (HJD-2,450,000)	5,581.520(3)	5,581.541(2)
$K_{\rm em}$ (km s^{-1})	104.2±3.8	100.8±3.3
γ (km s^{-1})	133.7±1.9	131.5±1.8
$f(M_X)$ ($M_\odot$)	$\geqslant$0.07	$\geqslant$0.04

lowing other LMXBs for which similar narrow features have been seen (e.g. Cornelisse et al. 2008), we think it likely that these lines arise on the irradiated surface of the donor star of MAXI J0556. Our period analysis shows that there are two possible orbital periods, 0.68d and 0.41d. From these periods we derived a radial velocity semi-amplitude of 101-104 km s^{-1}.

If the narrow components truly trace the irradiated companion we thereby obtain a lower limit to the mass-function of $f(M_X){=}M_X\sin^3 i/(1{+}q)^2{\geqslant}0.07 M_\odot$ (for $P_{\rm orb}{=}0.68$ day) or $\geqslant 0.04 M_\odot$ (for $P_{\rm orb}{=}0.41$ day), where i is the inclination and $q({=}M_X/M_{\rm donor})$ is the mass ratio. These mass functions are true lower-limits, since the lines should trace the radial velocity of the surface and not the center of mass of the donor star, and its true orbital velocity (K_2) should therefore always be higher (Muñoz-Darias et al. 2005).

One way we could further constrain the system parameters is by taking account of the X-ray properties of MAXI J0556, and in particular the reported eclipse-like features (Strohmayer 2011; Maitra et al. 2011a). Strohmayer (2011) reported that the eclipse was not total, nor "sharp", as might be expected if the X-ray source is obscured by the donor star. Belloni (private communication) confirmed this and suggested that these features more resemble dips, as are also observed in the high inclination system 4U 1254−69 (e.g. Diaz-Trigo 2009). In 4U 1254−69 these dips are thought to be caused by obscuration of the central X-ray source by the outer accretion disk edge, and the depth and strength strongly varies (sometimes the dips are even completely absent). Diaz-Trigo (2009) suggested the presence of a tilted/precessing accretion disk in 4U 1254−69 and if something similar is present in MAXI J0556 it implies a relatively high inclination.

The presence of such a tilted/precessing accretion disk would make MAXI J0556 similar to the dwarf novae that show superhumps, and could also explain why neither of our two potential orbital periods is close to any period suggested by the X-ray dips (Strohmayer 2011). Superhumps are commonly observed in dwarf novae during a superoutburst (see e.g. Patterson et al. 2005 for an overview), and are thought to be caused by an instability at the 3:1 resonance that forces the eccentric accretion disk to precess (e.g. Whitehurst 1988). Due to these deformations of the disk shape the photometric period in dwarf novae is typically a few percent longer than the orbital period, although superhump periods shorter than the orbital period have also been observed if the precessing disk is counter-rotating (Patterson et al. 2002).

Assuming that MAXI J0556 is a high inclination system (but not high enough for the donor to obscure the X-ray source) with a precessing accretion disk that sometimes partly obscures the central X-ray source, we can try to further constrain its system parameters. First of all, one of the original reported periods by Strohmayer (2011) must then be the superhump period. If the orbital period is 0.68 days (16 hrs) the superhump period would most likely be 0.58 days. Following Patterson et al. (2005), this would lead to an observed fractional period excess of ϵ=0.14 and suggests a mass ratio of $q\simeq$0.45. We note that this mass ratio is high for systems that typically show precession. However, Osaki (2005) pointed out that sufficiently hot accretion disks may expand beyond the 3:1 resonance radius and start precessing. Since MAXI J0556 is thought to be a Z-source and should have accretion rates close to Eddington (Homan et al. 2011), therefore it might be reasonable to expect a such hot accretion disk and therefore precession.

Using q=0.45 we can correct the velocity of the irradiated surface (our observed K_{em} of 104 km s^{-1}) to the center of mass velocity of the donor star using the K-correction developed by Muñoz-Darias et al. (2005). This would lead to a maximum K_2 velocity of 190 km s^{-1} (for a disk with an opening angle of 0°). Furthermore, q=0.45 suggests that eclipses by the secondary will occur for an inclination $\geqslant$72° (Paczynski 1974), and we use this as a first estimate of the inclination. Combining all these system parameters we obtain a mass for the compact object of $\simeq$1.2$M_\odot$, which is close to the canonical 1.4$M_\odot$ neutron star mass. We therefore believe that for a disk opening angle $\simeq$6° and a relatively high inclination it is also possible to obtain a 1.2-1.4$M_\odot$ compact object.

Given the system parameters above, we would need an inclination of $\simeq$40° to obtain a black hole with a mass of 3.2$M_\odot$. This is too low to realistically expect any dipping behavior.

For an orbital period of 0.4 days (with a superhump period of 9.33 hrs), and making the same assumptions as above, we would obtain a mass for the compact object of $\simeq$0.2$M_\odot$. Again, this would lead to unrealistically low inclinations to obtain any sensible compact object mass. We therefore think that our data are most consistent with a neutron star LMXB in a 0.68 days orbit and being observed at moderately high inclination.

5   CONCLUSIONS

We have presented the results of a spectroscopic campaign on the X-ray transient MAXI J0556 close to peak of outburst and have shown that strong N III emission lines are present in the spectrum, while C and O show no enhancement. This is in agreement with Maitra et al. (2011b) who have suggested an unusually high N/O abundance. Furthermore, all emission lines show a continuing decay over the $\simeq$one month of our observations, for which we have no good explanation.

Our radial velocity study has shown that only two orbital periods (0.68 and 0.41 days) are possible. From our dataset only we cannot distinguish the true orbital period so both periods are equally likely. We suggest that MAXI J0556 harbors a precessing accretion disk to explain not only the disappearance of the dip-like features observed in X-rays,

but also the discrepancy between the periods suggested by Strohmayer (2011) and ourselves. If the presence of a precessing accretion disk can be proved, then the X-ray dips suggest not only a reasonably high inclination but also that the longer period is most likely the true orbital period. This would imply that the compact object is a neutron star, strengthening the suggestion of Homan et al. (2011).

Since a superhump is usually not observed when a system is in quiescence, the scenario outlined above can only be confirmed with photometric observations obtained during a future outburst. Finding the true orbital period on the other hand can be obtained by observing MAXI J0556 when it is back in quiescence. With a quiescent optical magnitude of $R\simeq$20, it is easily accessible for both photometric and spectroscopic studies with medium-sized telescopes. Such studies would not only constrain the true orbital period and the radial velocity semi-amplitude of the center of mass of the donor star (instead of its irradiated surface), but hopefully constrain the inclination and binary mass ratio. This would offer solid dynamical constraints on the masses of the binary components, in order to verify that MAXI J0556 indeed harbors a neutron star and more accurately determine its mass.

REFERENCES

Belloni T., Motta S., Muñoz-Darias T., Stiele H., 2011, ATel, 3112

Charles P.A., & Coe M.J., 2006, in "Compact stellar X-ray sources", Cambridge Astrophysics series, No. 39, Cambridge University Press, p. 215

Coriat M., Tzioumis A.K., Corbel S., Fender R., Brocksopp C., Broderick J., Casella P., Maccarone T., 2011, ATel, 3119

Cornelisse R., Casares J., Steeghs D., Barnes A.D., Charles P.A., Hynes R. I., O'Brien K., 2007, MNRAS, 375, 1463

Cornelisse R., Casares J., Muñoz-Darias T., Steeghs D., Charles P.A., Hynes R.I., O'Brien K., Barnes A.D., 2008,

"A Population Explosion: The Nature & Evolution of X-ray Binaries in Diverse Environments", AIP Conf. Proc., Vol. 1010, p. 148

Diaz-Trigo M., Parmar A.N., Boirin L., Motch C., Talavera A., Balman S., 2009, A&A, 493, 145

Fender R.P., Russell D.M., Knigge C., Soria R., Hynes R.I., Goad M. 2009, MNRAS, 393, 1608

Goldoni P., Royer F., Francois P., Horrobin M., Blanc G., Vernet J., Modigliani A., Larsen J., 2006, SPIE, 6269, 80

Gray, D.F., 1992, "The Observation and Analysis of Stellar Photospheres", CUP, 20

Halpern J.P., 2011, ATel, 3104

Homan J., Linares M., van den Berg M., Fridriksson J. 2011, ATel, 3650

Horne K., 1986, PASP, 98, 609

van Hoof P.A.M., Verner D. 1997, in "Proceedings of the first ISO workshop on Analytical Spectroscopy", Eds. A.M. Heras, K. Leech, N.R. Trams and M. Perry, ESA Publications Division, 1997, p. 273

Kennea J.A., Evans P.A., Krimm H., Romano P., Mangano V., Curran P. Yamaoka K., 2011, ATel, 3103

Maitra D., Reynolds M.T., Miller J.M., Raymond J., 2011a, ATel, 3349

Maitra D., Miller J.M., Raymond J.C., Reynolds M.T. 2011b, accepted for ApJ Letters, astro-ph/1110.6918

Matsumura T., Negoro H., Suwa F., Nakahira S., Ueno S., Tomida H., Kohama M., Ishikawa M., et al. 2011, ATel, 3102

Muñoz-Darias T., Casares J., Martinez-Pais I.G., 2005, ApJ, 635, 502

Nelemans G., Jonker P.G., Marsh T.R., van der Klis M., 2004, MNRAS, 348, L7

Osaki, Y., in Proc. Japan Acad. Ser. B, Physical and Biological Sciences, Tokyo, p. 291

Paczynski B. 1974, A&A, 34, 161

Patterson J., Fenton W.H., Thorstensen J.R., Harvey D.A., Skillman D.R., Fried R.E., Monard B., et al., 2002, PASP, 114, 802

Patterson J., Kemp J., Harvey D.A., Fried R.E., Rea R., Monard B., Cook L.M., Skillman D.R., et al., 2005, PASP, 117, 1204

Psaltis D., 2006, in "Compact stellar X-ray sources", Cambridge Astrophysics series, No. 39, Cambridge University Press, p. 1

Russell D.M., Lewis F., Doran R., Roberts S., 2011, ATel, 3116

Scargle, J.D., 1982, ApJ, 263, 835

Shahbaz T., Smale A.P., Naylor T., Charles P.A., van Paradijs J., Hassall B.J.M., Callanan P., 1996, MNRAS, 282, 1437

Steeghs D., & Casares J., 2002, ApJ, 568, 273

Strohmayer T.E., 2011, ATel, 3110

Wade R.A., Horne K., 1988, ApJ, 324, 411

Whitehurst R., 1988, MNRAS, 232, 35